Confidential: not for distribution. Submitted to the American Astronomical Society for peer review 2010 April 8

WASP-22 b: A transiting "hot Jupiter" planet in a hierarchical triple system

P. F. L. Maxted[1], D. R. Anderson[1], M. Gillon[2,3], C. Hellier[1], D. Queloz[2], B. Smalley[1], A. H. M. J. Triaud[2], R. G. West[4], D. M. Wilson[1], S. J. Bentley[1], A. Collier Cameron[5], B. Enoch[5], L. Hebb[5], K. Horne[5], J. Irwin[6], T. A. Lister[7], M. Mayor[2], N. Parley[5], F. Pepe[2], D. Pollacco[8], D. Segransan[2], S. Udry[2], P. J. Wheatley[9]

ABSTRACT

We report the discovery of a transiting planet orbiting the star TYC 6446-326-1. The star, WASP-22, is a moderately bright (V=12.0) solar-type star ($T_{\rm eff} = 6000 \pm 100$ K, [Fe/H]= -0.05 ± 0.08). The lightcurve of the star obtained with the WASP-South instrument shows periodic transit-like features with a depth of about 1% and a duration of 0.14 d. The presence of a transit-like feature in the lightcurve is confirmed using z-band photometry obtained with Faulkes Telescope South. High resolution spectroscopy obtained with the CORALIE and HARPS spectrographs confirm the presence of a planetary mass companion with an orbital period of 3.533 days in a near-circular orbit. From a combined analysis of the spectroscopic and photometric data assuming that the star is a typical main-sequence star we estimate that the planet has a mass $M_{\rm p} = 0.56 \pm 0.02 M_{\rm Jup}$ and a radius $R_{\rm p} = 1.12 \pm 0.04 R_{\rm Jup}$. In addition, there is a linear trend of $40\,{\rm m\,s^{-1}\,y^{-1}}$ in the radial velocities measured over 16 months, from which we infer the presence of a third body with a long period orbit in this system. The companion may be a low mass M-dwarf or a second planet.

Subject headings: planetary systems

1. Introduction

The WASP project (Pollacco et al. 2006) is currently one of the most successful wide-area surveys designed to find exoplanets transiting bright stars (V < 12.5). Other succesful surveys include HAT-net (Bakos et al. 2004), XO (McCullough et al. 2005) and TrES (O'Donovan et al. 2006). There is continued interest in finding transiting exoplanets because they can be accurately characterized and studied in some detail, e.g., the mass and radius of the planet can be accurately measured. This gives us the opportunity to explore the relationships between the density of the planet and other properties of the planetary system, e.g., the semi-major axis, the spectral type of the star, the eccentricity of the orbit, etc. Given the wide variety of transiting planets being discovered and the large number of parameters that characterize them, statistical studies will require a large sample of sys-

[1]Astrophysics Group, Keele University, Staffordshire, ST5 5BG, UK

[2]Observatoire de Genève, Université de Genève, 51 Chemin des Maillettes, 1290 Sauverny, Switzerland

[3]Institut d'Astrophysique et de Géophysique, Université de Liège, Allée du 6 Août, 17, Bat. B5C, Liège 1, Belgium

[4]Department of Physics and Astronomy, University of Leicester, Leicester, LE1 7RH, UK

[5]School of Physics and Astronomy, University of St. Andrews, North Haugh, Fife, KY16 9SS, UK

[6]Department of Astronomy, Harvard University, 60 Garden Street, MS 10, Cambridge, Massachusetts 02138, USA

[7]Las Cumbres Observatory, 6740 Cortona Dr. Suite 102, Santa Barbara, CA 93117, USA

[8]Astrophysics Research Centre, School of Mathematics & Physics, Queen's University, University Road, Belfast, BT7 1NN, UK

[9]Department of Physics, University of Warwick, Coventry, CV4 7AL, UK

tems to identify and quantify the relationships between these parameters. These relationships can be used to test models of the formation, structure and evolution of short period exoplanets.

A particular puzzle related to the properties of some hot Jupiters is their very low densities. There is currently no generally agreed explanation for the existence of hot Jupiters with densities $5-10$ times lower than the density of Jupiter, e.g. WASP-17 b (Anderson et al. 2010), TrES-4 b (Mandushev et al. 2007) and WASP-12 b (Hebb et al. 2009). One possibility is that the planets are heated by tidal forces, and that these are driven by the presence of a third body in the system (Mardling 2007).

Here we report the discovery of a "hot Jupiter" system, WASP-22, identified using the WASP-South instrument and present evidence that it is a member of a hierarchical triple system.

2. Observations

The WASP survey is described in Pollacco et al. (2006) and Wilson et al. (2008) while a discussion of our candidate selection methods can be found in Collier Cameron et al. (2007), Pollacco et al. (2008), and references therein.

The WASP-South instrument consists of 8 cameras, each with a Canon 200-mm f/1.8 lens and a 2k×2k $e2V$ CCD detector. The star TYC 6446-326-1 (= 1SWASPJ 033116.32−234911.0) was observed 3133 times by one camera on the WASP-South instrument from 2006 August to 2007 January. A further 6282 obervations were obtained with the same camera from 2007 August to 2008 January. The star also appeared in the images obtained with a second camera during the second observing season, so a further 5889 observations were obtained with this camera during that interval.

The WASP-South lightcurves show transit-like features with a depth of approximately 0.012 magnitudes recurring with a 3.53-d period (Fig. 1) so we obtained spectroscopic observations using the CORALIE spectrograph on the Euler 1.2-m telescope and the HARPS spectrograph on the 3.6-m ESO telescope, both located at La Silla, Chile. We obtained 37 radial-velocity measurements during the interval 2008 August 27 to 2009 December 25 with CORALIE and 6 measurements with HARPS

Table 1: Radial velocity measurements.

BJD−2 400 000	RV (km s^{-1})	$\sigma_{\rm RV}$ (km s^{-1})	BS (km s^{-1})
CORALIE			
54704.8563	−7.236	0.013	0.005
54706.8761	−7.368	0.026	0.030
54708.8417	−7.189	0.011	−0.020
54709.7625	−7.320	0.019	−0.038
54710.7697	−7.291	0.024	0.046
54715.8843	−7.201	0.018	0.058
54716.8457	−7.262	0.041	−0.127
54717.7794	−7.386	0.041	0.034
54720.7520	−7.312	0.017	0.002
54721.8184	−7.289	0.019	0.028
54722.8233	−7.201	0.012	−0.033
54724.7367	−7.314	0.017	−0.011
54726.8108	−7.225	0.012	0.010
54729.8623	−7.206	0.013	−0.005
54731.8658	−7.345	0.012	−0.015
54740.7564	−7.199	0.020	−0.058
54834.5647	−7.304	0.018	0.014
54836.5707	−7.225	0.017	−0.019
54853.6313	−7.171	0.014	0.046
54854.6322	−7.275	0.013	0.018
54855.6091	−7.310	0.012	0.001
54860.5404	−7.183	0.013	0.051
54862.5589	−7.327	0.015	−0.046
54865.5628	−7.313	0.014	0.024
54879.5256	−7.280	0.017	−0.039
54880.5402	−7.273	0.021	0.033
54882.5242	−7.193	0.021	0.043
54885.5207	−7.159	0.016	−0.014
54886.5443	−7.299	0.017	−0.015
55095.8758	−7.308	0.013	0.013
55100.8593	−7.154	0.015	−0.002
55126.7935	−7.266	0.015	0.005
55128.7415	−7.169	0.016	0.006
55185.6618	−7.147	0.011	−0.007
55186.6153	−7.234	0.011	−0.025
55189.6571	−7.164	0.010	0.004
55190.6690	−7.284	0.011	−0.008
HARPS			
54743.7527	−7.1832	0.0029	0.0090
54746.7683	−7.2391	0.0026	0.0040
54749.7650	−7.2941	0.0024	0.0039
54750.6791	−7.1940	0.0029	0.0109
54754.7257	−7.1752	0.0025	0.0118
54755.7558	−7.2726	0.0032	0.0329

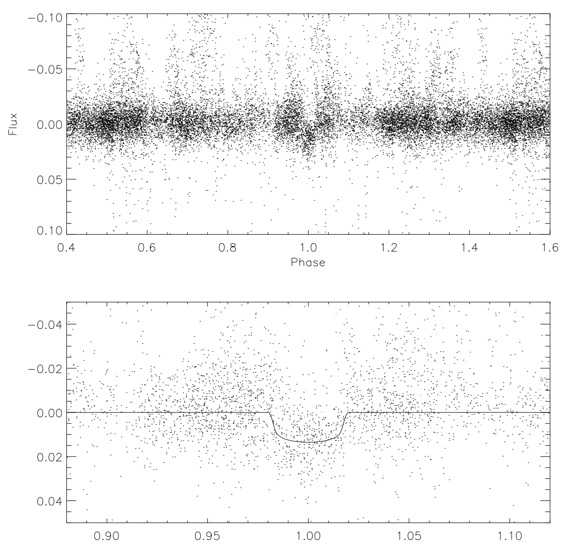

Fig. 1.— WASP-South photometry of WASP-22 folded on the orbital period $P = 3.532759$ d. Upper panel: all data. Lower panel: data within 0.12 phase units of mid-transit together with the model fit described in Section 3.1 (solid line).

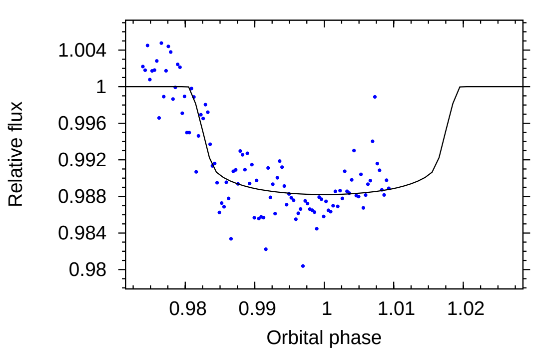

Fig. 2.— Faulkes Telescope South z-band photometry of WASP-22 (points) with the model fit described in Section 3.1 (solid line).

during the interval 2008 Oct 4 − 16. The measurements are given in Table 1, where we also provide the bisector span, BS, which measures the asymmetry of the cross-correlation function. The standard error of the the bisector span measurements is $2\sigma_{\rm RV}$.

We also obtained photometry of TYC 6446-326-1 and other nearby stars on 2009 August 8 using the LCOGT 2.0-m Faulkes Telescope South (FTS) at Siding Spring Observatory. The Merope camera we used has an image scale of 0.279 arcseconds/pixel when used in the 2x2 binning mode we employed. We used a Pan-STARRS[1] z-band filter to obtain 107 images covering one ingress of the transit. These images were processed in the standard way with IRAF[2] using a stacked bias image, dark frame, and sky flat. Minimal fringing was present in the z-band images due to the deep depletion CCD in the camera, so no fringe correction was applied. The DAOPHOT photometry package (Stetson 1987) was used to perform object detection and aperture photometry with an aperture size of 10 binned pixels in radius. The 5' $\times$ 5' field of view of the instrument contained 6 comparison stars that were used in deriving the differential magnitudes with a photometric precision of 3.1 mmag. The coverage of the out-of-transit phases is quite limited, but the data are sufficient to confirm that transit-like features seen in the WASP-South data are due to the star TYC 6446-326-1 and to provide better measurements of the depth of the transit and the duration of ingress than is possible from the WASP-South data (Fig. 2). We note that the star 1SWASP J033121.40-234857.8 77 arcsec from WASP-22 is also a variable star. This star showed a dip in brightness of about 0.01 magnitudes lasting about 100 minutes during our observation of WASP-22.

All photometric presented in this paper are available from the NStED database.[3]

[1] http://pan-starrs.ifa.hawaii.edu/public/design-features/cameras.html

[2] IRAF is distributed by the National Optical Astronomy Observatory, which is operated by the Association of Universities for Research in Astronomy (AURA) under cooperative agreement with the National Science Foundation.

[3] http://nsted.ipac.caltech.edu

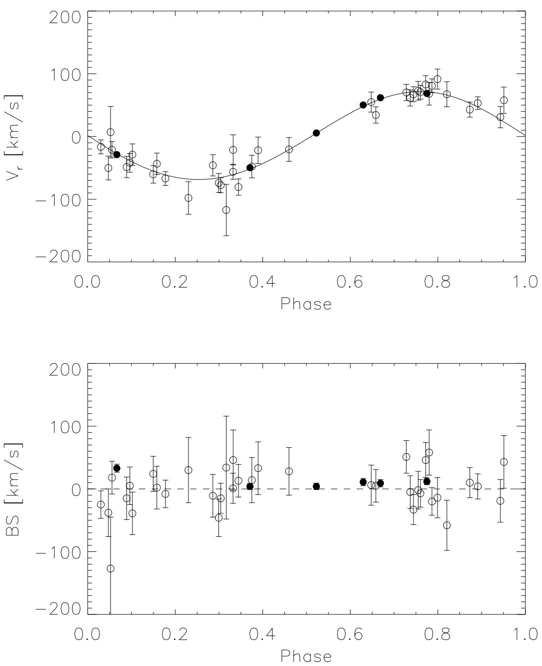

Fig. 3.— Radial velocity and bisector span measurements for WASP-22. Upper panel: Radial velocity relative to the centre-of-mass velocity including the long-term drift $\frac{d\gamma}{dt}$ (points with error bars) compared to our model for the spectroscopic orbit (solid line). Lower panel: bisector span measurements. Symbols are as for Fig. 4.

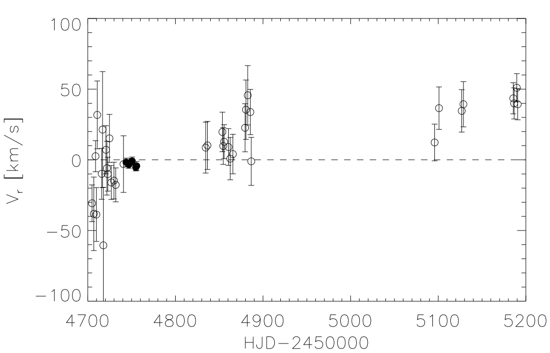

Fig. 4.— Residuals from a Keplerian orbit fit to our radial velocity data without a linear trend in the model. Data obtained with the HARPS spectrograph are plotted with filled circles, CORALIE data with open circles.

3. WASP-22 Stellar Parameters

The individual HARPS spectra of WASP-22 were co-added to produce a single spectrum with a typical S/N of around 100:1 that we have analysed to determine the atmospheric parameters of the star. The standard pipeline reduction products were used in the analysis.

The analysis was performed using the UCLSYN spectral synthesis package (Smith 1992; Smalley et al. 2001) and ATLAS9 models without convective overshooting (Castelli et al. 1997). The H_α line was used to determine the effective temperature ($T_{\rm eff}$), while the Na I D and Mg I b lines were used as surface gravity ($\log g$) diagnostics. The parameters obtained from the analysis are listed in Table 2.

The equivalent widths of several clean and unblended lines were measured. Atomic line data was mainly taken from the Kurucz and Bell (1995) compilation, but with updated van der Waals broadening coefficients for lines in Barklem et al. (2000) and $\log gf$ values from Gonzalez and Laws (2000), Gonzalez et al. (2001) or Santos et al. (2004). A value for microturbulence ($\xi_{\rm t}$) was determined from Fe I using the method of Magain (1984). The ionization balance between Fe I and Fe II and the null-dependence of abundance on excitation potential were used as an additional the $T_{\rm eff}$ and $\log g$ diagnostics (Smalley 2005).

We have determined the elemental abundances of several elements (also listed in Table 2) from their measured equivalent widths. The quoted error estimates include that given by the uncertainties in $T_{\rm eff}$, $\log g$ and $\xi_{\rm t}$, as well as the scatter due to measurement and atomic data uncertainties. There is no evidence from these data for any abundance anomolies in WASP-22.

The spectrum of WASP-22 shows a clear Li I 6708Å line with EW = 32 ± 1 mÅ, indicating an abundance of log n(Li/H) + 12 = 2.23 ± 0.08 dex. We have compared this lithium abundance to the relations between age, effective temperature and age by Sestito and Randich (2005). For stars with $T_{\rm eff} \approx 6000$ K we find that this lithium abundance implies a lower limit to the age of about 1 Gyr. However, Israelian et al. (2009) have noted that stars with planets have lower lithium abundances than normal solar-type stars, so the lithium abundance may not be a good age indicator for these stars.

The projected stellar rotation velocity ($v \sin i$) was determined by fitting the profiles of several unblended Fe I lines. A value for macroturbulence ($v_{\rm mac}$) of 4.5 km s^{-1} was assumed, based on the tabulation by Gray (2008), and an instrumental FWHM of 0.065Å, determined from the telluric lines around 6300Å. A best fitting value of $v \sin i$ = 3.5 ± 0.6 km s^{-1} was obtained.

We did not see any indication of additional spectral lines in the spectrum nor any trend in equivalent widths that might suggest contamination of the spectrum by another star. We estimate that the third body in this system discussed below contributes less than 5% of the light in the optical spectrum.

3.1. Planetary parameters

The amplitude of the radial velocity variation with the same period as the transit lightcurve (Fig. 3) and the lack of any correlation between this variation and the bisector span establish the presence of a planetary mass companion to this star (Queloz et al. 2001).

The CORALIE and HARPS radial velocity measurements were combined with the WASP-South and FTS photometry in a simultaneous Markov-chain Monte-Carlo (MCMC) analysis to find the parameters of the WASP-22 system. The shape of the transit is not well defined in the WASP-South or FTS photometry, so we have imposed an assumed main-sequence mass-radius relation as an additional constraint in our analysis of the data. The stellar mass is determined from the parameters $T_{\rm eff}$, $\log g$ and [Fe/H] using the procedure described by Enoch et al. (2010), based on the compilation of eclipsing-binary data by Torres et al. (2010). The code uses $T_{\rm eff}$ and [Fe/H] as MCMC jump variables, constrained by Bayesian priors based on the spectroscopically-determined values given in Table 2.

A careful analysis of the radial velocity data clearly shows a trend in the residuals as a function of time (Fig. 4). We therefore adapted our MCMC analysis to include an extra parameter, $\frac{d\gamma}{dt}$, which describes a linear trend in the centre-of-mass velocity of the star.

The parameters derived from our MCMC analysis are listed in Table 3. We found that we did not need to accont for any additional noise in the radial velocity data to due to stellar activity ("jitter"). The contribution to the total chi-squared from our 43 radial velocity measurements is 32.4. The surface gravity derived from our MCMC solution is consistent with the $\log g$ value from the analysis of the spectrum, but the large uncertainty on the latter value means that this is a rather weak constraint.

We have included the parameters $e \sin(\omega)$ and $e \cos(\omega)$ as free parameters in the solution because the orbit of the planet is not known to be circular, although the values of derived and their standard errors are quite consistent with this hypothesis. Imposing a circular orbit in the solution has a negligible effect on the value of the other parameters derived, but would reduce the estimated errors on these parameters, perhaps unrealisitically so.

4. Discussion

The third body we have detected from the linear trend in the radial velocities contributes less than 5% of the flux in the optical spectrum, so it is at least 3 magnitudes fainter than WASP-22 at V. This rules out the possibilty that the companion is K-type dwarf star, but leaves the possibility that the companion is an M-dwarf or a white dwarf. There is good agreement between the effective temperature we derive from the analysis of the optical spectrum and the effective temperature derived using the infrared flux method (Blackwell et al. 1979). We estimate that we would have been able detect a cool companion to WASP-22 if the 2MASS K_s-band magnitude (Skrutskie et al. 2006) were increased by more than 0.1 magnitudes. This also rules out a K-dwarf companion but not an M-dwarf companion or a white dwarf companion.

There are few direct constraints on the properties of the third body from the radial velocity data available to-date. The observation that the trend is linear over 16 months suggests that the orbital period is at least a few years. If the orbit of the third body is approximately circular and coplanar with the inner orbit with a period of several years and an amplitude comparable to the velocity range observed so far, then it is possible that the third body is a second planet, i.e., a configuration similar to the double-planet system HAT-P-13 (Bakos et al. 2009). Further radial velocity monitoring will be required to determine whether any or all of these assumptions is reasonable. This is certainly worth doing because the detection of a second planet in the WASP-22 system may make it possible to infer the interior structure of WASP-22 b using the method of Batygin et al. (2009). This method relies on an accurate measurement of the eccentricity for the orbit of the inner planet. The data available to-date are only of sufficient quality to state that the eccentricity of the orbit is small ($e \lesssim 0.06$) so more data of the quality we obtain from HARPS will be required to measure a precise value for the eccentricity of WASP-22 b's orbit.

The distance to WASP-22 is approximately 300pc so it may be possible to detect the companion directly if it is a M-dwarf using high-constrast, high-resolution imaging.

5. Conclusion

The star WASP-22 (TYC 6446-326-1) has a hot Jupiter companion. A long-term linear trend in the mean value of the radial velocity shows that WASP-22 has a distant companion, i.e., it is a hierarchical triple system. The properties of the third body are poorly constrained by the data available to-date, but it may be an M-dwarf, a white dwarf or a second planet.

WASP-South is hosted by the South African Astronomical Observatory and we are grateful for their ongoing support and assistance. Funding for WASP comes from consortium universities and from the UKs Science and Technology Facilities Council.

REFERENCES

Anderson, D. R. et al. 2010, ApJ, 709, 159

Bakos, G., Noyes, R. W., Kovács, G., Stanek, K. Z., Sasselov, D. D., and Domsa, I. 2004, PASP, 116, 266

Bakos, G. Á. et al. 2009, ApJ, 707, 446

Barklem, P. S., Piskunov, N., and O'Mara, B. J. 2000, A&AS, 142, 467

Batygin, K., Bodenheimer, P., and Laughlin, G. 2009, ApJ, 704, L49

Blackwell, D. E., Shallis, M. J., and Selby, M. J. 1979, MNRAS, 188, 847

Castelli, F., Gratton, R. G., and Kurucz, R. L. 1997, A&A, 318, 841

Collier Cameron, A. et al. 2007, MNRAS, 380, 1230

Enoch, B., Collier Cameron, A., Hebb, L., Parley, N. R. 2010, A&A, submitted.

Gonzalez, G. and Laws, C. 2000, AJ, 119, 390

Gonzalez, G., Laws, C., Tyagi, S., and Reddy, B. E. 2001, AJ, 121, 432

Gray, D. F. 2008, The Observation and Analysis of Stellar Photospheres (Cambridge University Press)

Hebb, L. et al. 2009, ApJ, 693, 1920

Israelian, G. et al. 2009, Nature, 462, 189

Kurucz, R. L. and Bell, B. 1995, Kurucz CD-ROM 23: Atomic line list (Smithsonian Astrophysical Observatory, Cambridge, MA)

Magain, P. 1984, A&A, 134, 189

Mandushev, G. et al. 2007, ApJ, 667, L195

Mardling, R. A. 2007, MNRAS, 382, 1768

McCullough, P. R., Stys, J. E., Valenti, J. A., Fleming, S. W., Janes, K. A., and Heasley, J. N. 2005, PASP, 117, 783

O'Donovan, F. T., Charbonneau, D., and Hillenbrand, L. 2006, in Bulletin of the American Astronomical Society, Vol. 38, Bulletin of the American Astronomical Society, p. 1212

Pollacco, D. et al. 2008, MNRAS, 385, 1576

Pollacco, D. L. et al. 2006, PASP, 118, 1407

Queloz, D. et al. 2001, A&A, 379, 279

Santos, N. C., Israelian, G., and Mayor, M. 2004, A&A, 415, 1153

Sestito, P. and Randich, S. 2005, A&A, 442, 615

Skrutskie, M. F. et al. 2006, AJ, 131, 1163

Table 3: System parameters for WASP-22. The planet equilibrium temperature is calculated assuming a value for the Bond albedo A= 0. **N.B.** an assumed main-sequence mass-radius relation is imposed as an additional constraint in this solution so the mass and radius of the star are not independent parameters – see Enoch et al. (2010) for details.

Parameter	Symbol	Value	Unit
Transit epoch (BJD)	T_C	2454780.2496 ± 0.0014	d
Orbital period	P	3.53269 ± 0.00001	d
Transit duration	T_{14}	0.137 ± 0.003	d
Planet/star area ratio	R_P^2/R_*^2	0.0104 ± 0.0004	
Impact parameter	b	0.13 ± 0.08	
Stellar reflex velocity	K_1	70.0 ± 1.7	$m\,s^{-1}$
Centre-of-mass velocity at time T_C	$\gamma_{CORALIE}(T_C)$	-7262 ± 2	$m\,s^{-1}$
Velocity offset, HARPS − CORALIE	$\gamma_{HARPS} - \gamma_{CORALIE}$	21 ± 2	$m\,s^{-1}$
Drift in centre-of-mass velocity	$\frac{d\gamma}{dt}$	40 ± 5	$m\,s^{-1}\,yr^{-1}$
Orbital separation	a	0.0468 ± 0.0004	AU
Orbital inclination	i	89.2 ± 0.5	°
Orbital eccentricity	e	0.023 ± 0.012	
Arg. of periastron	ω	27^{+51}_{-78}	°
	$e\cos(\omega)$	0.012 ± 0.011	
	$e\sin(\omega)$	0.006 ± 0.021	
Stellar mass	M_*	1.1 ± 0.3	$M_\odot$
Stellar radius	R_*	1.13 ± 0.03	$R_\odot$
Stellar surface gravity	$\log g_*$	4.37 ± 0.02	(cgs)
Stellar density	ρ_*	0.76 ± 0.06	$\rho_\odot$
Planet mass	M_P	0.56 ± 0.02	M_J
Planet radius	R_P	1.12 ± 0.04	R_J
Planet surface gravity	$\log g_P$	3.00 ± 0.03	(cgs)
Planet density	ρ_P	0.40 ± 0.04	ρ_J
Planet equil. temp.	T_P	1430 ± 30	K

Smalley, B. 2005, Memorie della Societa Astronomica Italiana Supplement, 8, 130

Smalley, B., Smith, K. C., and Dworetsky, M. M. 2001, UCLSYN User guide

Smith, K. 1992, Ph.D. thesis, University College, London

Stetson, P. B. 1987, PASP, 99, 191

Torres, G., Andersen, J., and Giménez, A. 2010, A&A Rev., 18, 67

Wilson, D. M. et al. 2008, ApJ, 675, L113

Table 2: Stellar parameters of WASP-22 from our spectroscopic analysis.

Parameter	Value
$T_{\rm eff}$ (K)	6000 ± 100
$\log g$	4.5 ± 0.2
$\xi_{\rm t}$ ($\rm km\,s^{-1}$)	1.2 ± 0.1
$v \sin i$ ($\rm km\,s^{-1}$)	3.5 ± 0.6
[Fe/H]	−0.05 ± 0.08
[Mg/H]	+0.06 ± 0.04
[Si/H]	+0.17 ± 0.11
[Ca/H]	+0.10 ± 0.11
[Sc/H]	+0.12 ± 0.12
[Ti/H]	+0.10 ± 0.07
[V/H]	+0.07 ± 0.09
[Cr/H]	0.00 ± 0.08
[Mn/H]	+0.02 ± 0.06
[Co/H]	+0.09 ± 0.13
[Ni/H]	+0.09 ± 0.06
log N(Li)	2.23 ± 0.08